AO 0235+164 AND SURROUNDING FIELD: SURPRISING *HST* RESULTS[1]

E. M. BURBIDGE, E. A. BEAVER, ROSS D. COHEN, V. T. JUNKKARINEN, AND R. W. LYONS

Center for Astrophysics and Space Sciences, University of California, San Diego, La Jolla, California 92093-0111
Electronic mail: mburbidge@ucsd.edu

Received 1996 June 25; revised 1996 September 5

ABSTRACT

Results obtained with the *Hubble Space Telescope* on the highly variable radio, x-ray, and γ-ray emitting QSO (or BL Lac object) AO 0235+164 are presented and analyzed. WFPC2 images were obtained in 1994 June, when AO 0235+164 was bright ($m\sim17$), and the results are described in Sec. 3. After subtraction of the PSF of the QSO, hereafter called AO following the nomenclature of Yanny *et al.* (1989), the companion object named A, 2″ south of AO, is discovered not to be an elliptical galaxy as hypothesized earlier, but to be an AGN object, with a central UV-bright point-source nucleus and faint surrounding nebulosity extending to AO. The second companion object 1.3″ east of AO discovered by Yanny *et al.* (1989) and named object A1, appears more like a normal spiral galaxy. We have measured the positions, luminosities, and colors of some 30 faint objects in the field around AO 0235+164; most are extended and may be star-forming galaxies in a loose group or cluster. Our most surprising result of the *HST* observations comes from FOS spectra obtained in 1995 July, discussed in Sec. 4. Because of a positioning error of the telescope and AO's faintness at that time ($m\sim20$), object A was observed instead of the intended target AO. Serendipitously, we discovered A to have broad deep BALQSO-type absorptions of C IV, Si IV, N V shortward of broad emissions. A is thus ejecting high velocity, highly ionized gas into the surrounding IGM. We discuss in Sec. 5 the relationship of the objects in the central 10″×10″ region around AO, where redshifts $z_e=0.94$, $z_a=0.524$, 0.851 in AO, $z_e=0.524$ and $z_{\rm BAL}=0.511$ in A, are found. We hypothesize that some of the 30 faint objects in the 77″×77″ field may be part of a large star-forming region at $z\sim0.5$, as suggested for a few objects by Yanny *et al.* (1989). The proximity of two highly active extragalactic objects, AO 0235+164 and its AGN companion A, is remarkable and one of the authors (EMB) suggests it may require consideration of a non-cosmological component of redshift in AO 0235+164.

1. INTRODUCTION

The Arecibo Occultation radio source AO 0235+164 (hereafter AO) is a highly variable radio, x-ray, and γ-ray emitting QSO which has been variously described as a blazar, BL Lac object, optically violent variable (OVV) QSO, and a high-polarization QSO (HPQ). Its V magnitude usually ranges from 17.5 to 19.5. Following a flare reaching $V=14.3$, Rieke *et al.* (1976) and Burbidge *et al.* (1976) measured two absorption-line systems $z_{a1}=0.524$ and $z_{a2}=0.851$ in its spectrum, but no emission lines were seen, so it was not possible to determine an emission-line redshift $z_{\rm em}$. Thus the designation BL Lac object seemed appropriate, although this designation was originally used to denote OVV-HPQ objects at the nuclei of elliptical galaxies (e.g., BL Lac itself, see also Burbidge & Hewitt 1987), and no elliptical galaxy was seen centered on AO.

Smith *et al.* (1977) showed that AO has a faint "companion" about 2 arcsec south, which has narrow emission lines of [O II], [O III], and Hβ at $z_e=0.524$, i.e., at $z_e=z_{a1}$, and suggested that all the absorption and emission might be produced by material associated with AO, whose emission-line redshift had not at that time been determined. Roberts *et al.* (1976) had measured complex 21 cm absorption in the radio spectrum of AO, centered at $z=0.524$, and Wolfe *et al.* (1982) showed this to be variable. Wolfe & Wills (1977), in an investigation of the physical conditions in the two absorption systems (both optical and 21 cm), concluded that the evidence available in 1977 was insufficient to show where the absorbing clouds lie along the line of sight.

Cohen *et al.* (1987), using data obtained in 1985 at Lick observatory with the CCD-grism spectrograph on the 3 m Shane telescope, determined an emission-line redshift $z_e=0.94$ based on weak lines of Mg II λ2800, [Ne V] λ3426, and [O II] λ3727. They also measured [O II] λ3727 and [O III] λ5007 at $z_e=0.524$ with the spectrograph slit centered on AO itself. They took this to be evidence of extended emission at $z=0.524$.

Yanny *et al.* (1989, hereafter YYG), using an interference filter at [O II] λ3727 $(1+z_{a1})$, discovered additional extended objects emitting [O II] λ3727 at $z=z_{a1}=z_{\rm em}=0.524$ in the field of AO as well as the Smith *et al.* "companion," which YYG named object A. The YYG object A1, 1.3 arcsec E of AO, is listed by them as being extended in the EW direction. Yanny *et al.* (1990) give R magnitudes of 20.9 and 22.3 for A and A1, respectively. Two of the additional objects, YYG

[1]Based on observations with the NASA/ESA *Hubble Space Telescope*, obtained at the Space Telescope Science Institute, which is operated by AURA, Inc., under NASA Contract No. NAS 5-26555.

 0004-6256/96/112(6)/2533/8/$10.00

TABLE 1. Journal of *HST* observations.

Date	Instrument	Filter/ Wavelength range	Exposure Time (s)
1994 Jun 26	WFPC2	F450W	1200
1994 Jun 26	WFPC2	F702W	600
1994 Jun 26	WFPC2	F785LP	600
1995 Jul 19	FOS G160L 0.″86 round	1600-2430 Å	11280
1995 Jul 19	FOS G270H 0.″86 round	2210-3230	4770

B, 6 arcsec SW of AO, and YYG C, 26 arcsec SW of AO, have z_e=0.524 confirmed by slit spectroscopy (Stickel *et al.* 1988; Yanny 1990). These authors discussed the nature of the objects at z_e=0.524 and the implications of large star-forming regions at this redshift producing heavy elements, specifically oxygen, and their relation to the highly active QSO AO.

AO is a strong x-ray source with an x-ray spectrum which Madejski (1994) showed could be fitted by a synchrotron power-law $F_E \propto E^{\alpha}$, plus absorption that could be due to the K edges of O, Ne, Mg and the L edge of Fe at z_e=0.524. This implies a large column of neutral H, as is expected from the 21 cm observations. Madejski *et al.* (1996) have confirmed this absorption with *ROSAT* and ASCA observations, and obtained γ-ray data with GRO/EGRET which showed AO to be a strong emitter; γ-ray variability was not detected.

In Sec. 2 we describe the *HST* observations and data analysis: the WFPC2 observations in Sec. *2.1* and the Faint Object Spectrograph (FOS) observations in Sec. *2.2*. In Sec. 3 we present the results of the WFPC2 observations: for the central object AO itself in Sec. *3.1*, for the companion object A in Sec. *3.2*, for the second faint companion object A1 in Sec. *3.3*, and for a large number of faint objects in the field surrounding AO in Sec. *3.4*. In Sec. 4 we present the results of the *HST*/FOS spectra. Discussion of the results and conclusions are given in Sec. 5.

2. OBSERVATIONS WITH THE *HUBBLE SPACE TELESCOPE*

Both AO and object A, assumed to produce most of the absorption in AO, were on our *HST*/GTO program, to

(a) observe AO with the FOS to measure Lyman absorption at z_a=0.524 for combining with the 21 cm absorption to get spin temperature, element abundances, and physical conditions in the absorbing gas;

(b) obtain WFPC2 images of the field of AO and the companions, specifically for the morphology of object A.

Observations obtained in 1994 and 1995 are listed in Table 1. Instrumental details and data reduction procedures follow.

2.1 WFPC 2 Observations

Images of AO and the surrounding field were obtained with the *HST* and the WFPC2 camera on 1994 June 26 (program 5096). AO was placed near the center of chip 3. Two exposures were obtained through the F450W, F702W, and F785LP filters, each lasting 600, 300, and 300 s, respectively. The *HST* pipeline-reduced exposures for each filter were averaged together using the STSDAS WFPC task "combine." For this task, we set crreject=3, to reject many of the cosmic rays seen in the data.

AO was bright at the time of observation and must be subtracted prior to any interpretations or measurements of the objects within its immediate surroundings. Following the approach of Yanny *et al.* (1989), we assumed the central part of the AO object is dominated by a QSO point spread function. We used the "Tiny Tim" optical simulation code (version 4.0, Krist 1993) to create a point spread function (PSF), sampled every 0.1 pixel at the approximate position of AO. To include CCD subpixel variations and scattered light within the CCD, we convolved the PSF with the CCD pixel spatial response function (Krist, private communication). An optimal PSF for subtraction from the AO image was calculated by iteratively varying the PSF centroid position and peak intensity at the re-sampled original pixel scale until achieving a minimum χ^2 in an annulus which excluded the saturated core.

Some 30 objects in the field of AO were identified visually on the combined F702W image. Most of these objects appear extended; they are listed and discussed in Sec. *3.4*. In addition, modulations exist in the background that may also be faint objects, but the exposures were insufficient to judge whether these are real or to determine their nature.

Photometry on each of the combined images and PSF-corrected region around AO was carried out using aperture photometry programs written in the Lick Observatory VISTA command language, augmented by Barlow (1993). These programs determine the total number of counts above the background in a circle centered on the centroid of the selected image derived iteratively or the current cursor position, if no well-defined center exists. The average background is determined using pixels in an annulus surrounding the integration region for the object. Regions in the background that had obvious contamination were omitted from the background calculation, as were significant cosmic rays that had not been rejected by the combine procedure. The size of each object and its background annulus is determined by the user.

The integrated counts for each object were converted to flux and m_{ν} in the *HST* filter system using the revised photflam values given by Whitmore (1995).

2.2 Faint Object Spectrograph Observations

Observations were obtained on 1995 July 19 with the G160L and G270H gratings and the Red Digicon of the FOS through the 0.″86 circular aperture (program 6217). The G160L exposure lasted 11 280 s and covered the wavelength range from 1600 to 2425 Å at low resolution ($R \approx 250$). The G270H exposure took 4770 s and covered the wavelength range 2225 to 3275 Å at moderate resolution ($R \approx 1300$). Since the spectrum was sampled at one-quarter diode spacing, the actual exposure time per data point is one quarter of the values shown above.

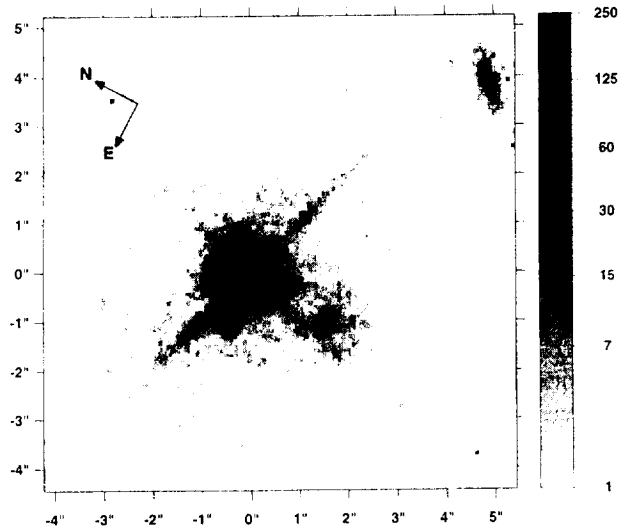

FIG. 1. Central 10″×10″ of field around AO 0235+164, the sum of two exposures obtained with the *Hubble Space Telescope* WFPC2 camera through the F702W filter. AO is the bright (m_v=17) central object with diffraction spikes. Companion object A is 2″ S of AO, with its point-source core and surrounding luminosity that is most extended on the NW side between the diffraction spikes of AO. Second companion object A1 is 1.3 E of AO, just S of the E diffraction spike. Galaxy No. 9 in Table 2 (z=0.524) is seen in the top right corner. A greyscale based on the relative counts is shown at the right.

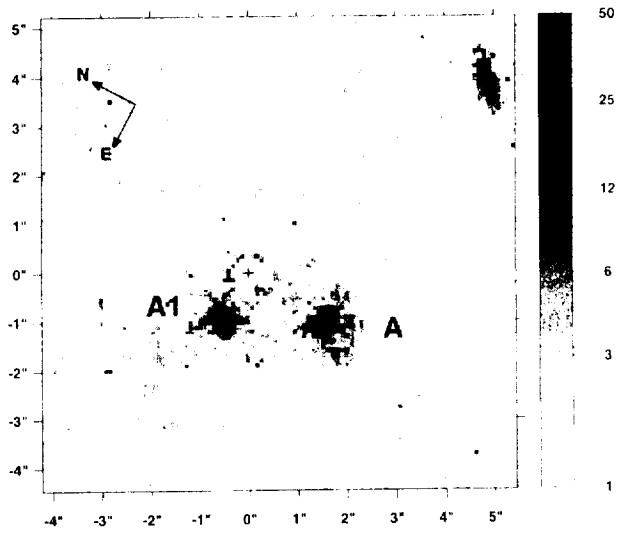

FIG. 2. *HST*/WFPC2 image of the central field around AO 0235+164 as in Fig. 1, with the PSF of the bright central object AO and its diffraction spikes removed. The cross marks the center of the subtracted PSF, and companion objects A and A1 are marked. The strong core of object A, extended luminosity S of the core, and the arms or plumes towards AO are clearly seen. The second companion object A1 E of AO is also clearly seen: it has an extended luminosity ~0.5 in diameter without a bright nucleus but with extensions NW and SE giving it the appearance of an edge-on Sa galaxy. A number of pixels with counts above background are seen in an area 2″×1.5 NE of AO and A1.

While the intended target of the exposures was AO itself, the actual target observed was object A. This resulted because a small initial pointing error placed both AO and A in the target acquisition aperture. While it had been bright a year earlier, on the day of the FOS observations AO was as faint as it had ever been observed, approximately V=20.5. This magnitude was comparable to that of object A, and the target acquisition algorithm selected A as the observation target.

The spectra were reduced by standard procedures giving flux as a function of wavelength.

3. RESULTS OF WFPC2 IMAGES

Figures 1 and 2 show the central 10″×10″ region containing AO and nearby objects through the F702W filter, as observed and summed with the "combine" task, and with the PSF subtracted, as described in Sec. *2.1*. Although the diffraction spikes of AO are largely removed by the subtraction, positive and negative residuals remain, indicating that perfect subtraction is not possible with our PSF. Results obtained from these images are described in the following paragraphs.

3.1 Central Object AO

There is residual luminosity around the center of AO (marked with a cross in Fig. 2), after subtraction of the PSF with its diffraction spikes, and pixels with counts above background lie in an area 2×1.5 arcsec that crosses the NE diffraction spike. High-resolution imaging at a time when the central source of AO is faint is needed to reveal the structure of this extended luminosity.

3.2 Companion Object A

Figures 1 and 2 show clearly that A is not, as has sometimes been assumed, a normal elliptical galaxy. On the F450W image (not shown) it has essentially PSF dimensions with very faint extended emission, while the F702W image shows a central point source and faint surrounding luminosity. This luminosity has a well-defined edge 0.5 S of the core, and there appear to be two curved plumes or arms on the opposite side of the core, SW of AO and between the diffraction spikes of AO.

To estimate the proportion of counts in this surrounding nebulosity relative to the total counts that we can assign to A (core plus nebulosity) we have subtracted the central point source by a procedure similar to but somewhat more subjective than that used to subtract the PSF from AO. We find that the extended emission comprises 0.34 and 0.64 of the total in the F450W and F702W images, respectively. At the redshift z=0.524, these filters correspond to emitted radiation centered on 3000 and 4600 Å, respectively. Thus the extended emission is stronger in the blue than in the UV relative to the core emission, as expected since the core has AGN characteristics as described in Sec. 4.

3.3 Companion Object A1

This object is shown well in Fig. 2. It has no central point source like *A*, and appears to be elongated ~2 arcsec in a NW/SE direction. The brightest area has diameter ~0.5 arcsec.

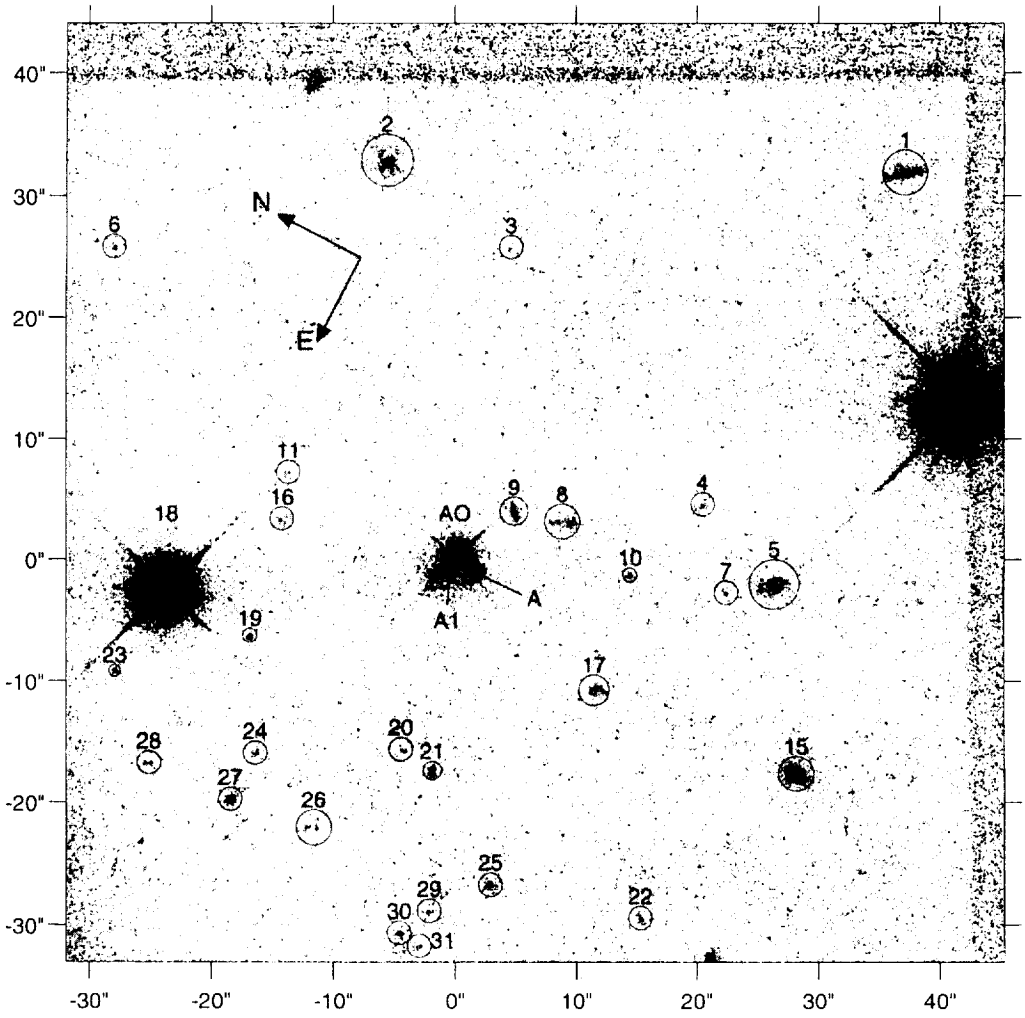

FIG. 3. *HST*/WFPC2 image of the ~77″×77″ area through the F702W filter centered approximately on AO. The faint objects listed in Table 2 are numbered, with the "apertures" used in measuring each object superimposed. Note the jet extending NE from No. 8 in the direction of No. 9, as described in Sec. *3.4*, also the double and possible multiple galaxies are mentioned there.

3.4 Other Objects in the Field of AO

Figure 3, representing an area of sky ~77″×77″ through the F702W filter centered approximately on AO, shows the field surrounding AO, and the faint objects mentioned in Sec. *2.1*, identified and measured as described in Sec. *2.1*, with the "apertures" used for each object superimposed. Table 2 lists the objects accepted as real, i.e., objects detected at better than 4σ significance through any filter. They are listed in order by R.A., with the coordinates relative to AO ($\Delta\alpha$ and $\Delta\delta$), their magnitudes in the WFPC2 instrumental system, any previous identifications, references, redshifts and comments on their appearance in Fig. 3. One of these objects, No. 9, seen clearly in Figs. 1 and 2, is a spiral galaxy with $z=0.525$. In some cases, the positions were determined by eye because the objects were too faint to determine centroids. Since the plate scale of the WFPC2 is 0.097 arcsec per pixel, any position errors will be small since we are measuring relative positions only.

The errors shown in the magnitudes were derived using photon statistics. Additional fainter objects for which the measurements are not good enough to be included in Table 2 are clearly present in the field.

For comparison with the data in Table 2, we have examined the other chips of our WFPC2 image, and counted the number of nonstellar objects with 4σ or better detection. There are 19 such objects in WF#2 and 13 in WF#4. A few objects are seen in WF#1, the PC-CCD, but the signal level is lower and the area of sky covered is much less. WF#3, covering the area SE of AO, contains an excess number of objects, and the higher density region appears to run off of the chip. Until we obtain spectra and redshifts of these faint objects, and (as we hope) obtain a WFPC2 image of the area adjoining the edges of WF#3, we cannot estimate the size of what appears to be an extended group.

Some of the objects shown in Fig. 3 are particularly interesting, e.g., objects 8 and 9 in Table 2. There appears to be a jet extending NE from No. 8, in the direction of No. 9. SFK show our No. 8 as joined to their object G1, which is our No. 9 (YYW object B). Examination of Fig. 3 shows that No. 17 is a possible multiple galaxy, and Nos. 26 and 28 appear to be double galaxies, and are listed as such in Table 2.

In Fig. 4 we have plotted $(m_{450}-m_{702})$ vs $(m_{702}-m_{785})$ for the faint extended objects in Table 2. We have also plotted, over the redshift range $0<z<1.6$, the calculated colors

TABLE 2. Relative coordinates and instrumental magnitudes for objects in WFPC2 field around AO 0235+164.

ID	Coordinates		m_ν (WFPC2)			Published IDs		Redshift	comment
	$\Delta\alpha$ (")	$\Delta\delta$ (")	m_{450}	m_{702}	m_{785}	YY[c,e]	SFK[d]		
1	-46.37	-18.67	23.1± 0.2	21.14± 0.04	20.29± 0.06	9			edge-on galaxy
2	-27.20	20.59	22.9± 0.2	21.29± 0.06	20.65± 0.07	10			extended, featureless galaxy
3	-25.53	7.96	24.4± 0.3	24.0± 0.3	23.1± 0.3				point-like source
4	-13.83	-16.46	24.9± 0.5	22.9± 0.1	23.0± 0.2				galaxy
5	-10.57	-24.97	22.6± 0.1	21.41± 0.06	21.04± 0.10	C		0.525[f]	extended, featureless galaxy
6	-10.14	37.41	26.0± 1.2	23.5± 0.2	22.6± 0.2				point-like source
7	-8.07	-21.68	25.3± 0.6	24.0± 0.3	23.1± 0.3				point-like source
8	-7.02	-6.60	25.2± 0.9	22.12± 0.08	21.30± 0.09				galaxy, bright nucleus with jet
9	-5.84	-2.65	23.3± 0.1	21.37± 0.03	20.86± 0.04	B	G1	0.525[d,f]	edge-on galaxy
10	-5.64	-13.83	25.2± 0.4	22.61± 0.06	21.30± 0.04				point-like source
11	-0.00	15.83	25.6± 0.8	23.9± 0.3	23.1± 0.3				faint galaxy
12	0.00	0.00	---	---	---	AO		0.94[b]	
13	0.21	-1.95	21.40± 0.01	20.61± 0.01	20.33± 0.01	A		0.524[a,f]	
14	1.08	-0.07	22.46± 0.01	21.33± 0.01	21.21± 0.02	A1		0.524?[f]	
15	2.67	-33.85	21.80± 0.03	19.69± 0.01	19.21± 0.01	D	G2	0.065[d]	bright galaxy
16	3.73	14.44	24.2± 0.2	23.1± 0.1	22.7± 0.2				faint galaxy
17	4.31	-15.58	23.2± 0.1	22.36± 0.10	21.8± 0.1	I1			multiple galaxy?
18	13.36	20.24				S1			K-type star[g]
19	13.65	12.20	23.8± 0.1	22.96± 0.08	22.6± 0.1				compact galaxy
20	16.23	-3.40	23.8± 0.2	24.0± 0.3	22.8± 0.2				faint galaxy
21	16.73	-6.58	24.2± 0.3	22.09± 0.05	21.32± 0.06				galaxy
22	19.39	-27.80	24.2± 0.2	23.1± 0.1	23.2± 0.3				galaxy
23	21.40	20.82	25.6± 0.4	23.8± 0.1	23.5± 0.2				galaxy
24	22.03	7.08	26.3± 1.6	23.6± 0.2	22.7± 0.2				galaxy
25	22.81	-15.22	25.9± 1.1	22.56± 0.07	21.50± 0.06				galaxy
26	25.47	0.01	23.3± 0.2	22.8± 0.1	22.5± 0.2				double galaxy
27	26.61	7.29	22.42± 0.06	20.20± 0.01	19.24± 0.01	E			M-type star[g]
28	26.97	14.69	24.0± 0.2	23.9± 0.2	22.9± 0.2				double galaxy
29	27.26	-11.70	24.7± 0.4	23.7± 0.2	23.3± 0.3				galaxy
30	29.89	-10.38	24.5± 0.3	22.49± 0.07	21.67± 0.07				galaxy
31	30.03	-12.23	24.8± 0.4	23.4± 0.2	22.4± 0.1				galaxy

[a] Smith, Burbidge & Junkkarinen 1977
[b] Cohen et al. 1987
[c] Yanny, York & Gallagher 1989
[d] Stickel, Fried & Khur 1988
[e] Yanny, York & Williams 1990
[f] Yanny 1990
[g] Barlow, Burbidge, Cohen & Junkkarinen 1987

in our filter bands for the four galaxy types (irregular, Scd, Sbc, and old stellar population of M31 and M81) of Coleman *et al.* (1980). The measured colors of the extended objects are consistent with the spectra of normal galaxies at $z \leq 1$. The objects range between $19.7 \leq m_{702} \leq 24.0$. At $z = 0.524$, objects of median brightness ($m_{702} = 22.8$) would correspond to $M_B = -19.1$, while the faintest measured objects would have $M_B = -17.9$, similar to the luminosity of the Large Magellanic Cloud. Note the points for A and A1, that both have colors similar to low-z Irr-Scd galaxies, although these colors are uncertain because of errors inherent in the subtraction of the PSF of AO. The blue color of A is primarily due to its UV-strong nucleus, since the surrounding nebulosity is redder than the nucleus, as described in Sec. *3.2*.

4. RESULTS OF FOS SPECTRA

The spectra of object A are shown in Figs. 5 and 6. To our surprise, these spectra show that object A has broad absorptions displaced to the short-wavelength side of the C IV, Si IV, and N V emission lines, like some of the less extreme BALQSOs. The emission lines of Lyα, C IV λ1549, and C III λ1909 have broad emission wings characteristic of a QSO, and the Lyα emission has a sharp central spike, but no broad absorption.

The wavelengths measured from the maxima and minima of the flux and the derived redshifts of emission and absorp-

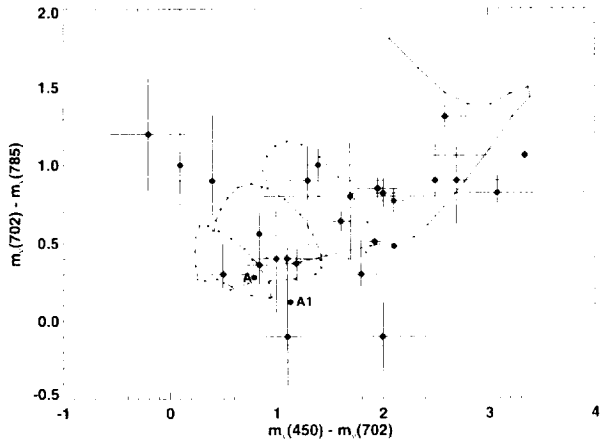

FIG. 4. Colors of the objects listed in Table 2 which are not known to be stars. The errors are derived from photon statistics. The large errors in $m_\nu(450) - m_\nu(702)$ for some objects are dominated by the errors in $m_\nu(450)$. Superimposed are the synthetic colors for four galaxy types (Coleman *et al.* 1980): Im (dot-dash), Scd (dash), Sbc (dot), and an old stellar population (solid). The curves are calculated for $0 \leq z \leq 1.6$ and marked every 0.1z, increasing in a counterclockwise direction.

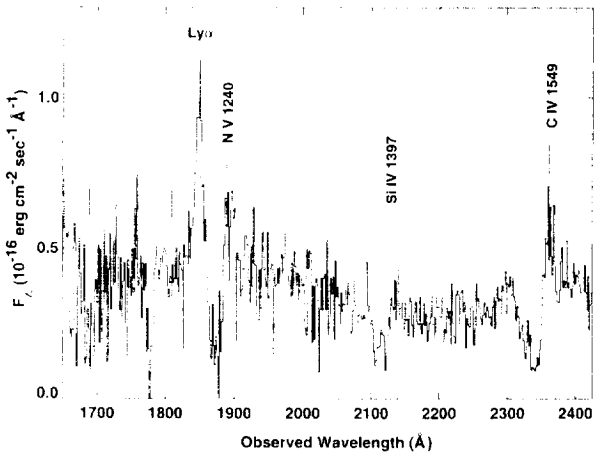

FIG. 5. *HST*/FOS spectrum of the object A 2″ S of the BL Lac object AO, obtained with the G160L grating and 0″.86 circular aperture, with identifications of C IV, Si IV, N V, Lyα marked. Note the BAL-type strong absorption troughs shortward of the emission line peaks. Note that Lyα has no broad absorption trough; three narrow absorptions shortward of Lyα emission are marked. The dotted line at the bottom marks the 1σ error array.

tion features are given in Table 3. Due to the faintness of A, the S/N is low and the wavelengths measured are necessarily rough.

The C IV λ1549 BAL is asymmetric; the red (low velocity) side is steeper than the blue and the blue edge of the trough shows some possible structure. The C IV λ1549 absorption in velocity units extends from roughly 1500 to 6000 km s^{-1} using the peak of C IV emission for the systemic emission redshift. The observed frame equivalent widths of the N V λ1240, Si IV λ1397, and C IV λ1549 BALs are approximately 19, 11, and 25 Å, respectively. The absorptions are not black and thus either the optical depths are modest or the BAL region does not completely cover the continuum and emission line source. The signal to noise is not sufficient to determine if partial covering is present for the Si IV λ1397 doublet absorption features while for C IV λ1549 and N V λ1240 the G160L resolution ($R \approx 250$) is not sufficient to resolve the doublets. Even at higher resolution and signal to noise it may not be possible to estimate the covering because BAL troughs in general are typically too smooth to show the doublet structure in C IV and N V. The spectrum of object A is similar to the spectra of the majority of BALQSO in that the troughs are not completely black, the BAL features are steeper at the low velocity edge, and the strong absorption features are all high ionization metals. The minimum absorption velocities, the velocity widths, and the equivalent widths of the absorption features are at the low end of what is observed for BALQSOs (Weymann *et al.* 1991) and object A is a borderline BALQSO by the formal balnicity index definition used by Weymann *et al.* (The Weymann *et al.* balnicity index is a quantitative equivalent width measure in velocity units of the total strength of BAL features in a QSO spectrum.) The balnicity index for the C IV absorption in object A (roughly 500 km s^{-1} with a large uncertainty) is small compared to the balnicity index of most other BALQSOs because the absorption is near the systemic velocity and relatively narrow. Even though the balnicity index is small, the absorption characteristics of object A are most like those of typical high ionization BALQSOs.

TABLE 3. Wavelengths and redshifts of emission and absorption lines in *HST*/FOS spectra of object A.

$\lambda_{obs}(em)$	ID	z_e	$\lambda_{obs}(abs)$	ID	z_a
1849.7	Lyα 1216	0.522	1689.0	Lyα 1216?	(0.389)
1891.0	NV 1240	0.525	1777.6	Lyα 1216?	(0.462)
2362.0	CIV 1549	0.525	1809.7	Lyα 1216?	(0.489)
2495.5	HeII 1640	0.521	1871.8	NV 1240	0.509
2534.7	OIV 1663	0.524	2106.0	SiIV 1391	0.511
2907.0	CIII] 1909	0.523	2121.5	SiIV 1403	0.512
			2340.0	CIV 1549	0.511
	Average	0.523	Average	(NV, SiIV, CIV)	0.511

UV spectra in some Seyfert 1 nuclei show variable P Cygni absorptions shifted as much as 2000 km s^{-1} shortward of the emission lines (Ulrich & Boisson 1983; Voit *et al.* 1987; Ulrich 1988), but those shown in the literature usually resemble "associated absorption systems" rather than BALs. Of the six Seyfert 1 galaxies with *IUE* spectra studied by Ulrich (1988), the only spectrum that looks at all like our data on object A is PG 1411+442, notably in its weakness of Si IV λ1397 emission and the absence of broad Lyα absorption. Malkan *et al.* (1987) discuss PG 1411+442 as a low redshift (and low luminosity) BALQSO. Compared to object A, the equivalent width of C IV λ1549 absorption in PG 1411+442 is somewhat less (12 vs 16 Å rest) and the maximum outflow velocity is also less (4000 vs 6000 km s^{-1}). Although about ten times less luminous than PG 1411+442, object A has somewhat stronger absorption features. (The absolute magnitude of 1411+442 is $M_B = -23.7$ ($H_0 = 50$ km s^{-1} Mpc^{-1}), while object A has $M_B = -21.3$). The BAL phenomenon apparently extends to relatively low luminosity AGNs, although, as mentioned in Malkan *et al.* (1987), very high outflow velocities may require more luminous QSOs.

Figures 5 and 6 show that there is no broad absorption that would correspond to Lyα at the mean $z_a = 0.511$ given in Table 3. There are three narrow absorptions, marked in Figs. 5 and 6, whose wavelengths are listed in Table 3 with the redshifts that they would have if they were all due to Lyα.

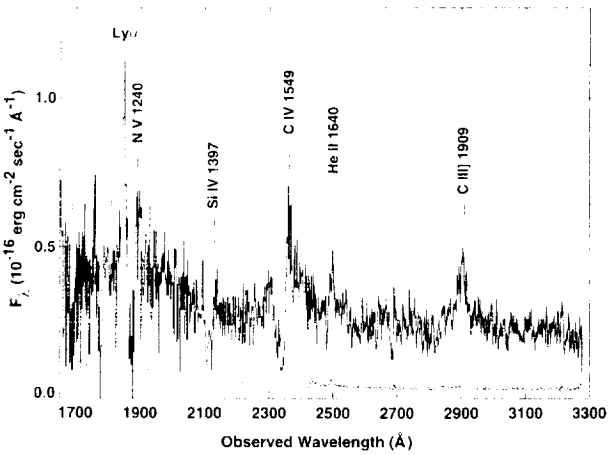

FIG. 6. Both spectra of object A obtained with the *HST*/FOS 0″.86 circular aperture and gratings G160L and G270H, joined where indicated by the dotted line. The G270H data have been smoothed by a 7-point boxcar; the corresponding error data have been divided by $\sqrt{7}$. Note the broad emission wings of C IV λ1549, He II λ1640 and C III λ1909.

The strongest, at 1689 Å, resembles a Ly limit absorption edge, but if this were a Ly limit it would have a redshift $z_a=0.852$, coincidentally close to the second absorption-line redshift observed in the spectrum of AO, $z_{a2}=0.851$ (Rieke *et al.* 1976; Burbidge *et al.* 1976; Wolfe & Wills 1977). If it is a Lyα line, it gives $z=0.389$.

5. DISCUSSION AND CONCLUSIONS

The most interesting discovery revealed by our *HST* observations concerns the nature of object A in the remarkable configuration of objects AO, A, A1 in the $10''\times10''$ region shown in Figs. 1 and 2. The *HST*/WFPC2 observations show that object A is not a "normal" elliptical galaxy but is an AGN surrounded by faint nebulosity. The broad strong high-ionization absorptions revealed by the *HST*/FOS spectra suggest that A should be classified as a BALQSOs with a small balnicity index (Weymann *et al.* 1991).

However, the magnitude $m_{702}=20.6$ in Table 2 gives an absolute magnitude $M_B=-21.3$ for $z=0.524$ ($H_0=50$ km s^{-1} Mpc^{-1}, $q_0=0.5$), which is a value more characteristic of Seyfert 1 nuclei than of QSOs. In any case, A is a very active object and is apparently ejecting N^{3+},C^{3+},Si^{3+} at high velocity into the intergalactic medium.

We do not have spectra of the curved plumes or arms extending NW from A and lying SW of AO as seen in Fig. 2. If A is a Seyfert 1 spiral galaxy, it should have a gaseous disk extending beyond AO, with enough low-ionization gas to produce the 21 cm and Mg, Mn, Fe absorption at $z=0.524$ in the radio and optical spectrum of AO. If the spectra of A had extended further into the UV, one might have seen a Ly limit edge at $z=0.524$. We expect to see a damped Lyα line at $z=0.524$ in the spectrum of AO itself, as indicated by the *IUE* observations of Snijders *et al.* (1982), when we succeed in observing its UV spectrum with *HST*.

Since A has such remarkable AGN properties, it may well be emitting x-ray and radio emission itself, but its proximity to the powerful and variable radiation at these wavelengths from AO precludes, with the resolution presently available, an investigation into this possibility. Murphy *et al.* (1993) have shown that AO at 1.64 GHz is extended over $\sim7''$ in a NW/SE direction, but the radio alignment is not in the direction of the AO-A alignment. Earlier, Jones *et al.* (1984) published VLBI data on AO at 1.3 cm with a resolution <0.2 milliarcsec, showing AO's core to have very small angular size, but we have found no data that can be related to the position of A.

Our WFPC2 data show the YYG object A1 is clearly separated from AO and A (Fig. 2). It has no central point source like A. Possibly it is a galaxy at the redshift $z=0.851$ seen in absorption in the spectrum of AO, but the narrow-band filter observations of YYG suggest that it has $z\approx0.524$. If so, with $M_B=-20.6$, it may also produce absorption at this redshift in the spectrum of AO, and might contribute to the complex H I 21 cm absorption studied by Wolfe *et al.* (1982). New observations at 21 cm would be interesting, to compare with the Wolfe *et al.* data and to check for further variations in intensity of the 21 cm components.

It will be interesting to obtain spectra of the faint extended objects listed in Table 2. How many have redshifts $z\sim0.52$? Do the spectra of any show star-forming properties? The existence of an extended loose group of young star-forming galaxies at this low redshift, as suggested by YYG and SFK, would have important cosmogonic implications, especially as A has an AGN nucleus and is ejecting high-velocity ionized gas into the surrounding medium.

The $10''\times10''$ region centered on AO is a remarkable configuration involving three redshifts: $z=0.524$, 0.851, 0.94, as well as z(BAL)=0.511. What is the probability of such a configuration? If A is taken to be a QSO, the probability of another chance configuration of two QSOs with different redshifts, separated by $<5''$, in addition to the three already known, is extremely small (cf. Burbidge *et al.* 1996). If A is taken to be a Seyfert 1 galaxy with an extraordinarily active nucleus, the probability of such an alignment would also seem very small, although the frequency of such galaxies out to $z>0.5$ is unknown. One is left with either a very contrived gravitational lensing possibility, needing a better model than that of Schneider (1993), or the unpopular situation of non-cosmological redshifts.

Clearly the whole field around AO 0235+164 needs further study. We plan further UV spectra of AO and A when STIS is installed on the *HST*. Observation of the spectrum of the fainter companion A1 1.3 arcsec from AO may be possible although difficult with the Keck 10 m telescope and LRIS. Improved ground-based imaging of the field is planned, as well as Keck/LRIS spectroscopy of the faint objects in the field discussed in Sec. *3.4*. We note that Fig. 3 shows that the objects listed in Table 2 cluster SE of AO, and the group runs off the edges of the WF#3. It will be interesting to obtain a WFPC2 image of the adjoining area to determine the extent of this apparent group.

This research has been carried out with the support of NASA Grant No. NAG5-1630, and has made use of the NASA/IPAC Extragalactic Database (NED which is operated by the Jet Propulsion Laboratory, California Institute of Technology, under contract with the national Aeronautics and Space Administration). We thank Dr. Fred Hamann for his helpful comments on this manuscript.

REFERENCES

Barlow, T. A. 1993, Ph.D. dissertation, University of California, San Diego, p. 57

Barlow, T. A., Burbidge, E. M., Cohen, R. D., & Junkkarinen, V. T. 1987 (private communication)

Burbidge, E. M., Caldwell, R. D., Smith, H. E., Liebert, J., & Spinrad, H. 1976, ApJ, 205, L117

Burbidge, G., & Hewitt, A. 1987, AJ, 93, 1

Burbidge, G., Hoyle, F., & Schneider, P. 1996, A&A (in press)

Cohen, R. D., Smith, H. E., Junkkarinen, V. T., & Burbidge, E. M. 1987, ApJ, 318, 577

Coleman, G. D., Wu, C-C., & Weedman, D. W. 1980, ApJS, 43, 393

Jones, D. L., Bååth, L. B., Davis, M. M., & Unwin, S. C. 1984, ApJ, 284, 60

Krist, J. 1993, in Astronomical Data Analysis Software and Systems II, ASP Conf. Proc. 52, edited by R. J. Hanisch, R. J. V. Brissenden, and J. Barnes (ASP, San Francisco), p. 530
Madejski, G. 1994, ApJ, 432, 554
Madejski, G., Takahashi, T., Tashiro, M., Kubo, H., Hartman, R., Kallman, T., & Sikora, M. 1996, ApJ, 459, 156
Malkan, M. A., Green, R. F., & Hutchings, J. B. 1987, ApJ, 322, 729
Murphy, D. W., Browne, W. A., & Perley, R. A. 1993, MNRAS, 264, 298
Rieke, G. H., Grasdalen, G. L., Kinman, T. D., Hintzen, P., Wills, B. J., & Wills, D. 1976, Nature, 260, 754
Roberts, M. S., Brown, R. L., Brundage, W. D., & Rots, A. H. 1976, AJ, 81, 293
Schneider, P. 1993, Gravitational Lenses in the Universe, Proceedings of the 31st Liège International Astrophysical Colloquium, edited by J. Surdej *et al.* (Institut d'Astrophysique, Liège), p. 41
Smith, H. E., Burbidge, E. M., & Junkkarinen, V. T. 1977, ApJ, 218, 611
Snijders, M. A. J., Boksenberg, A., Penston, M. V., & Sargent, W. L. W. 1982, MNRAS, 201, 801
Stickel, M., Fried, J. W., & Kuhr, H. 1988, A&A, 198, L13 (SFK)
Ulrich, M.-H. 1988, MNRAS, 230, 121
Ulrich, M.-H., & Boisson, C. 1983, ApJ, 267, 515
Voit, G. M., Shull, J. M., & Begelman, M. C. 1987, ApJ, 316, 573
Weymann, R. J., Morris, S. L., Foltz, C. B., & Hewett, P. C. 1991, ApJ, 373, 23
Whitmore, B. 1995, in Calibrating the Hubble Space Telescope: Post Servicing Mission, edited by A. Koratkar and C. Leitherer (STScI, Baltimore), p. 269
Wolfe, A. M., & Wills, B. J. 1977, ApJ, 218, 39
Wolfe, A. M., Davis, M. M., & Briggs, F. H. 1982, ApJ, 259, 495
Yanny, B. 1990, ApJ, 351, 396
Yanny, B., York, D. G., & Gallagher, J. S. 1989, ApJ, 338, 735 (YYG)
Yanny, B., York, D. G., & Williams, T. B. 1990, ApJ, 351, 377 (YYW)